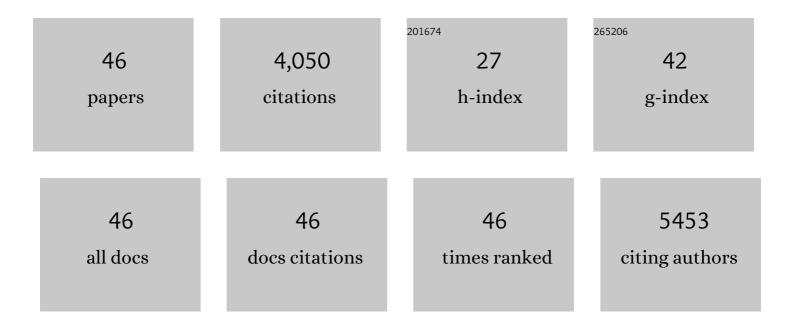
## Lan Sun

## List of Publications by Year in descending order

Source: https://exaly.com/author-pdf/7255547/publications.pdf Version: 2024-02-01



#	Article	IF	CITATIONS
1	p–n Heterojunction photoelectrodes composed of Cu2O-loaded TiO2 nanotube arrays with enhanced photoelectrochemical and photoelectrocatalytic activities. Energy and Environmental Science, 2013, 6, 1211.	30.8	483
2	Inorganic-modified semiconductor TiO <sub>2</sub> nanotube arrays for photocatalysis. Energy and Environmental Science, 2014, 7, 2182-2202.	30.8	461
3	Some Critical Structure Factors of Titanium Oxide Nanotube Array in Its Photocatalytic Activity. Environmental Science & Technology, 2007, 41, 4735-4740.	10.0	274
4	Nitrogen-doped TiO2 nanotube array films with enhanced photocatalytic activity under various light sources. Journal of Hazardous Materials, 2010, 184, 855-863.	12.4	240
5	Ultrasound aided photochemical synthesis of Ag loaded TiO2 nanotube arrays to enhance photocatalytic activity. Journal of Hazardous Materials, 2009, 171, 1045-1050.	12.4	223
6	Effects of the Structure of TiO[sub 2] Nanotube Array on Ti Substrate on Its Photocatalytic Activity. Journal of the Electrochemical Society, 2006, 153, D123.	2.9	200
7	Fabrication of uniform Ag/TiO2 nanotube array structures with enhanced photoelectrochemical performance. New Journal of Chemistry, 2010, 34, 1335.	2.8	181
8	Photoelectrocatalytic properties of Ag nanoparticles loaded TiO2 nanotube arrays prepared by pulse current deposition. Electrochimica Acta, 2010, 55, 7211-7218.	5.2	175
9	Optimized porous rutile TiO2 nanorod arrays for enhancing the efficiency of dye-sensitized solar cells. Energy and Environmental Science, 2013, 6, 1615.	30.8	160
10	Superhydrophilic–superhydrophobic micropattern on TiO2 nanotube films by photocatalytic lithography. Electrochemistry Communications, 2008, 10, 387-391.	4.7	147
11	A facile hydrothermal deposition of ZnFe2O4 nanoparticles on TiO2 nanotube arrays for enhanced visible light photocatalytic activity. Journal of Materials Chemistry A, 2013, 1, 12082.	10.3	119
12	Ultrasound-assisted synthesis and visible-light-driven photocatalytic activity of Fe-incorporated TiO2 nanotube array photocatalysts. Journal of Hazardous Materials, 2012, 199-200, 410-417.	12.4	118
13	Reduced platelet adhesion and improved corrosion resistance of superhydrophobic TiO2-nanotube-coated 316L stainless steel. Colloids and Surfaces B: Biointerfaces, 2015, 125, 134-141.	5.0	101
14	Oneâ€Dimensional Densely Aligned Perovskiteâ€Decorated Semiconductor Heterojunctions with Enhanced Photocatalytic Activity. Small, 2015, 11, 1436-1442.	10.0	86
15	Nonepitaxial growth of uniform and precisely size-tunable core/shell nanoparticles and their enhanced plasmon-driven photocatalysis. Journal of Materials Chemistry A, 2016, 4, 7190-7199.	10.3	85
16	An ultrasound-assisted deposition of NiO nanoparticles on TiO2 nanotube arrays for enhanced photocatalytic activity. Journal of Materials Chemistry A, 2014, 2, 8223.	10.3	82
17	Acid Orange II degradation through a heterogeneous Fenton-like reaction using Fe–TiO <sub>2</sub> nanotube arrays as a photocatalyst. Journal of Materials Chemistry A, 2015, 3, 8537-8544.	10.3	80
18	N-doped TiO2 nanotube array photoelectrode for visible-light-induced photoelectrochemical and photoelectrocatalytic activities. Electrochimica Acta, 2013, 108, 525-531.	5.2	79

Lan Sun

#	Article	IF	CITATIONS
19	Electrochemical construction of Z-scheme type CdS–Ag–TiO2 nanotube arrays with enhanced photocatalytic activity. Electrochemistry Communications, 2011, 13, 1469-1472.	4.7	78
20	Efficient visible light-induced photoelectrocatalytic hydrogen production using CdS sensitized TiO <sub>2</sub> nanorods on TiO <sub>2</sub> nanotube arrays. Journal of Materials Chemistry A, 2015, 3, 22218-22226.	10.3	72
21	Sonoelectrochemical synthesis of highly photoelectrochemically active TiO <sub>2</sub> nanotubes by incorporating CdS nanoparticles. Nanotechnology, 2009, 20, 295601.	2.6	71
22	Core–Shell–Satellite Plasmonic Photocatalyst for Broad-Spectrum Photocatalytic Water Splitting. , 2021, 3, 69-76.		59
23	Controllable construction of ZnO/TiO2patterningnanostructures by superhydrophilic/superhydrophobic templates. New Journal of Chemistry, 2010, 34, 44-51.	2.8	44
24	Enhanced photoelectrocatalytic hydrogen production activity of SrTiO 3 –TiO 2 hetero-nanoparticle modified TiO 2 nanotube arrays. International Journal of Hydrogen Energy, 2015, 40, 9704-9712.	7.1	44
25	SERS study of Ag nanoparticles electrodeposited on patterned TiO <sub>2</sub> nanotube films. Journal of Raman Spectroscopy, 2011, 42, 986-991.	2.5	42
26	Direct Z-scheme WO3- nanowire-bridged TiO2 nanorod arrays for highly efficient photoelectrochemical overall water splitting. Journal of Energy Chemistry, 2021, 59, 721-729.	12.9	42
27	Enhanced visible light photoelectrocatalytic activity over Cu <sub>x</sub> Zn <sub>1â^'x</sub> In <sub>2</sub> S <sub>4</sub> @TiO <sub>2</sub> 2 hetero-structures. Journal of Materials Chemistry A, 2017, 5, 1292-1299.	10.3	37
28	Multi-functional hybrid protonated titanate nanobelts with tunable wettability. Soft Matter, 2011, 7, 6313.	2.7	28
29	3D Heterostructured Ti-Based Bi <sub>2</sub> MoO <sub>6</sub> /Pd/TiO <sub>2</sub> Photocatalysts for High-Efficiency Solar Light Driven Photoelectrocatalytic Hydrogen Generation. ACS Applied Energy Materials, 2019, 2, 558-568.	5.1	23
30	Fe3+-Doped TiO2 Nanotube Arrays on Ti-Fe Alloys for Enhanced Photoelectrocatalytic Activity. Nanomaterials, 2016, 6, 107.	4.1	22
31	Room temperature synthesis of CdS nanoparticle-decorated TiO2 nanotube arrays by electrodeposition with improved visible-light photoelectrochemical properties. Electrochemistry Communications, 2016, 63, 56-59.	4.7	22
32	LaFeO 3 nanoparticle-coupled TiO 2 nanotube array composite with enhanced visible light photocatalytic activity. Materials Letters, 2018, 216, 1-4.	2.6	22
33	Controllable incorporation of CdS nanoparticles into TiO2 nanotubes for highly enhancing the photocatalytic response to visible light. Science in China Series B: Chemistry, 2009, 52, 2148-2155.	0.8	20
34	Controllable degradation of medical magnesium by electrodeposited composite films of mussel adhesive protein (Mefp-1) and chitosan. Journal of Colloid and Interface Science, 2016, 478, 246-255.	9.4	18
35	Rational Construction of LaFeO3 Perovskite Nanoparticle-Modified TiO2 Nanotube Arrays for Visible-Light Driven Photocatalytic Activity. Coatings, 2018, 8, 374.	2.6	18
36	Electrochemical synthesis of perovskite LaFeO <sub>3</sub> nanoparticle-modified TiO <sub>2</sub> nanotube arrays for enhanced visible-light photocatalytic activity. New Journal of Chemistry, 2019, 43, 16506-16514.	2.8	18

Lan Sun

#	Article	IF	CITATIONS
37	Preparation of Acid-Resisting Ultramarine Blue by Novel Two-Step Silica Coating Process. Industrial & Engineering Chemistry Research, 2011, 50, 7326-7331.	3.7	16
38	Synthesis of Surface-Oxygen-Vacancy-Rich (GaN) <sub>0.5</sub> (ZnO) <sub>0.5</sub> Particles with Enhanced Visible-Light Photodegradation Performance. Inorganic Chemistry, 2020, 59, 7012-7026.	4.0	14
39	High-efficiency photoelectrochemical hydrogen generation enabled by p-type semiconductor nanoparticle-decorated n-type nanotube arrays. RSC Advances, 2017, 7, 17551-17558.	3.6	13
40	ZnGaNO Photocatalyst Particles Prepared from Methane-Based Nitridation Using Zn/Ga/CO <sub>3</sub> LDH as Precursor. Inorganic Chemistry, 2018, 57, 9412-9424.	4.0	13
41	Al2O3-TiO2 composite oxide films on etched aluminum foil fabricated by electrodeposition and anodization. Science China Chemistry, 2011, 54, 1558-1564.	8.2	10
42	Heterostructured Ternary In <sub>2</sub> 0 <sub>3</sub> â^'Agâ^'TiO <sub>2</sub> Nanotube Arrays for Simulated Sunlightâ€Ðriven Photoelectrocatalytic Hydrogen Generation. ChemElectroChem, 2021, 8, 577-584.	3.4	7
43	Tuning Ag morphology on TiO2 nanotube arrays by pulse reverse current deposition for enhanced plasmon-driven visible-light response. Journal of Applied Electrochemistry, 2017, 47, 959-968.	2.9	3
44	Heterojunctions: One-Dimensional Densely Aligned Perovskite-Decorated Semiconductor Heterojunctions with Enhanced Photocatalytic Activity (Small 12/2015). Small, 2015, 11, 1435-1435.	10.0	0
45	Automatic identification of ramie and cotton fibers based on iodine blue reaction, Part I: the optimum conditions for the iodine blue reaction of cellulose. Textile Reseach Journal, 2016, 86, 848-855.	2.2	0
46	A Scientometric Analysis of Aerogel Research in 1996-2015. , 2017, , .		0

46 A Scientometric Analysis of Aerogel Research in 1996-2015. , 2017, , .